

Calculation of the $Z + \text{jet}$ cross section including transverse momenta of initial partons

M. Deak^a, A. van Hameren^a, H. Jung^b,
A. Kusina^a, K. Kutak^{a,d}, M. Serino^c

^a Institute of Nuclear Physics, Polish Academy of Sciences,
ul. Radzikowskiego 152, 31-342, Cracow, Poland

^b DESY, Hamburg, Germany

^c Department of Physics,
Ben Gurion University of the Negev,
Beer Sheva 8410501, Israel

^d Theoretical Physics Department, CERN,
1211 Geneva 23, Switzerland

September 12, 2018

Abstract

We perform calculations of $Z + \text{jet}$ cross-section taking into account the transverse momenta of the initial partons. Transverse Momentum Dependent (TMD) parton densities obtained with the Parton Branching method are used and higher order corrections are included via TMD parton showers in the initial state. The predictions are compared to measurements of forward $Z + \text{jet}$ production of the LHCb collaboration at $\sqrt{s} = 7$ TeV. We show that the results obtained in k_T -factorization are in good agreement with results obtained from a NLO calculation matched with traditional parton showers. We also demonstrate that in the forward rapidity region, k_T -factorization and hybrid factorization predictions agree with each other.

1 Introduction

The Large Hadron Collider (LHC) opened opportunities to explore kinematic regions where particles produced in high-energy collisions possess large transverse momenta and a wide range of available rapidities. The production of electroweak bosons and jets is a vital test of the Standard Model. Furthermore, studies of the associated production of electroweak bosons and jets provide important insights into the transverse partonic structure of hadrons. In particular, motivated by earlier studies [1–5], one can use recent theoretical and technical advancements to study in more detail Transverse Momentum Dependent Parton Densities (TMDs) [6].

Final states of the Z +jet type, being a combination of colored and colourless partons and particles, give the opportunity for investigations which complement the results obtained in studies of pure jet final states [7]. This is because final state rescatterings due to soft color exchanges have less impact on the properties of the produced final state as compared to pure jet final states.

This work focuses on predictions using k_T -factorization [8] (also referred to as High Energy Factorization) as implemented in the parton-level event generator KATIE [9] combined with a TMD initial state parton shower implementation in new version of CASCADE [10, 11] compared to Z +jet measurements of the LHCb collaboration [12].

The k_T -factorization formula for the inclusive cross section schematically reads

$$\sigma = \int \frac{1}{F} dPS \sum_{i,j} \mathcal{A}_i(x_1, k_{T1}, \mu_F) \otimes |ME|^2 \otimes \mathcal{A}_j(x_2, k_{T2}, \mu_F), \quad (1)$$

where F is the flux, PS is the final state phase space and ME is the partonic matrix element. The TMD parton distributions $\mathcal{A}_i(x, k_T, \mu_F)$ depend for a parton of type i on the longitudinal momentum fraction x , the factorization scale μ_F and the transverse momentum k_T , i.e. the momentum perpendicular to the collision axis of the colliding partons. The formula is valid when x is not too small and additional effects from gluon recombinations can be neglected [13, 14]. The matrix elements in the formula above are efficiently calculated numerically using helicity methods [15, 16] and recursion relation as implemented in KATIE [9], giving the same results as using Lipatov’s effective action [17].

The TMD parton densities can be defined by introducing operators whose expectation values count the number of partons and their evolution is given by renormalization of divergences either in rapidity or transversal momentum. One can also construct TMDs starting from the collinear parton densities by “unfolding” them by the Watt-Kimber-Martin-Ryskin prescription [18, 19]. In the Parton Branching (PB) method [20, 21], which will be used in this article, the TMD is constructed by a parton branching algorithm to solve the DGALP evolution equations. The starting distributions are obtained from a fit to inclusive DIS cross section measurements [22], using NLO splitting functions. The advantage of using PB-TMDs is that once integrated over the transverse momentum the collinear parton density functions are obtained, which is essential for a consistent comparison between k_T -factorization and collinear

approaches. The PB-TMDs are well suited to construct initial state parton showers [11] in such a way, that the kinematics of the hard process are fixed and no kinematic corrections are applied when the parton shower is added, as opposed to what is typically done in genuine collinear physics based Monte Carlo generators. With the PB-TMDs one can address observables initiated by initial state off-shell quarks and, in the end, perform a Monte Carlo simulation of the whole event, e.g. for a process

$$P_A + P_B \longrightarrow Z/\gamma^* + j + X \rightarrow \mu^+ \mu^- + j + X, \quad (2)$$

where P_A and P_B are the colliding protons which produce the intermediate state with one jet j and one Z/γ^* boson and other unobserved particles in a state X . We compare the prediction with a measurement obtained by LHCb [12], where the Z -boson decay into muon pairs was studied.

2 Results

We present results computed in the framework of k_T -factorization and Hybrid Factorization and compare them to the recent Z + jet measurements of LHCb [12]. We use KATIE [9] in order to produce parton-level events with off-shell initial-state momenta. These events are then further processed by CASCADE [10] with its extension for a complete initial state parton shower for all flavours, as described in Ref. [11]. The final state parton shower and hadronization are performed by PYTHIA [23]. We also use calculations performed in collinear factorization, with parton showers added, in LO for $Z+1$ jet and at NLO for $Z+2$ jets using POWHEG [24] together with PYTHIA [25] for parton showering, multi-parton interaction and hadronization. For all calculations we use two-loop α_s with $\alpha_s(m_Z) = 0.118$. The parton branching TMDs [22] (more specifically PB-NLO-2018-Set 2), available in TMDlib [26], are used for k_T dependent calculations while for the hybrid approach (with one on-shell and one off-shell initial parton) and the collinear approach we use the HERAPDF20_NLO_EIG collinear PDFs [27]. The PB-NLO-2018 TMDs, once integrated over k_T , reproduce HERAPDF20_NLO, by construction. The analysis of the final state particles is performed with the Rivet framework [28].

From all the distributions measured by LHCb [12] we will concentrate on the $\Delta\phi$ and p_T^Z distributions, for which going beyond the collinear approximation is most relevant.

2.1 Parton level results

We start by discussing results of calculations performed at the parton level (without any showering or hadronization, but with the decay $Z/\gamma^* \rightarrow \mu^+ \mu^-$), by convolving the TMD densities with the matrix elements, as schematically described by Eq. (1).

In Fig. 1 we show distributions of $\Delta\phi$ and p_T^Z calculated using two off-shell initial-state partons for two different cuts on the jet transverse momentum (as used by LHCb): $p_T^{\text{jet}} > 10$ GeV and $p_T^{\text{jet}} > 20$ GeV. The renormalization and factorization scale was set

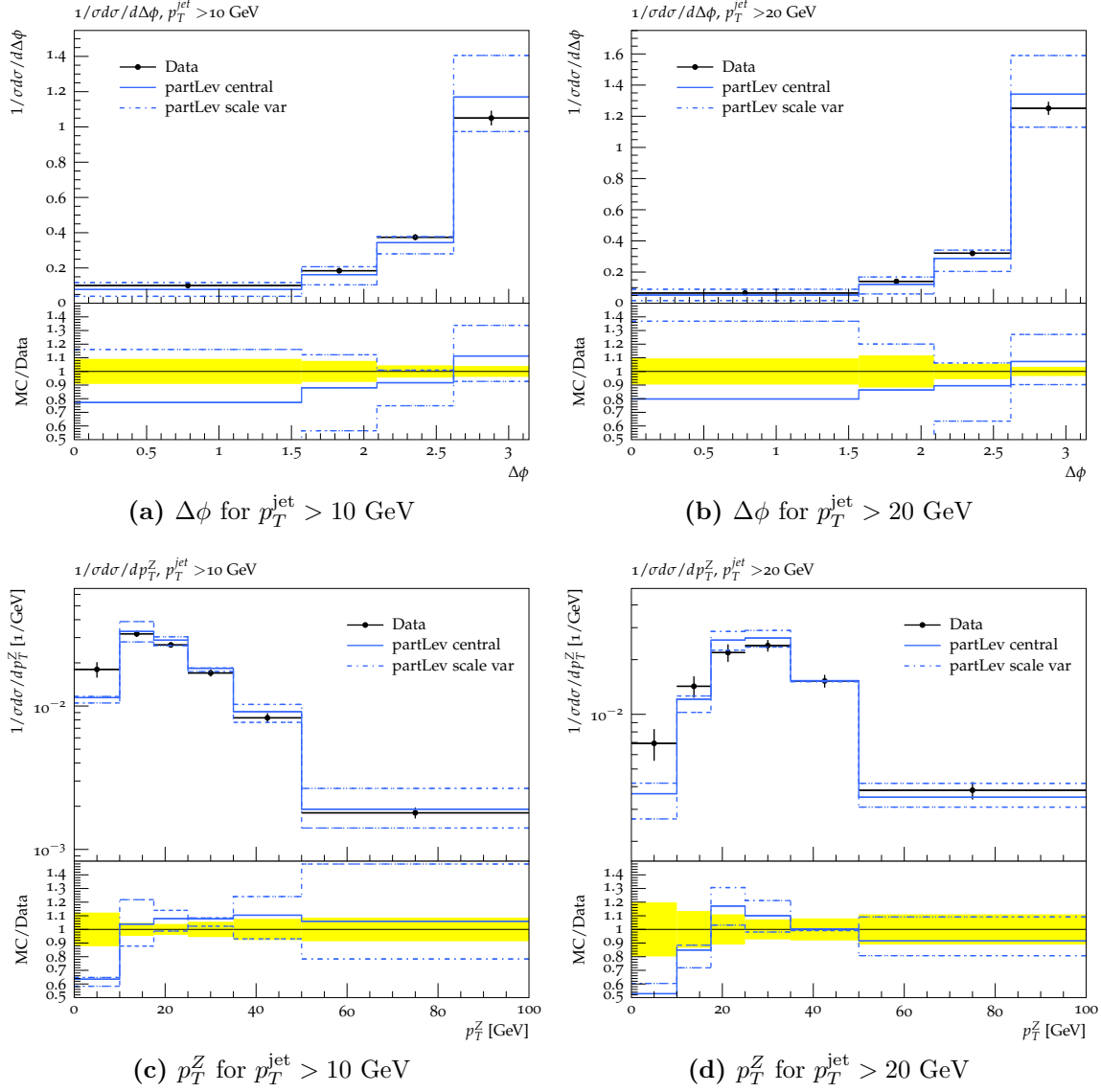


Figure 1: Scale variation for $\Delta\phi$ and p_T^Z distributions calculated at the parton level (without any showers) using a factorization/renormalization scale $\mu = \sqrt{m_Z^2 + (p_T^{\text{jet}})^2}$. Compared to the LHCb measurements [12].

to $\mu = \sqrt{m_Z^2 + (p_T^{\text{jet}})^2}$, which is varied by a factor of two up and down in order to estimate the scale uncertainty. We can see that for both cut choices the description of the $\Delta\phi$ distribution is very good and the data lie within the scale uncertainties. The measurement of p_T^Z is also well described, with the exception of the lowest p_T -region, where the data are underestimated. This is the region that is driven by the initial state transverse momentum described by the TMDs. In a collinear parton-level $2 \rightarrow 2$ calculation the region below the p_T^{jet} cut would be empty.

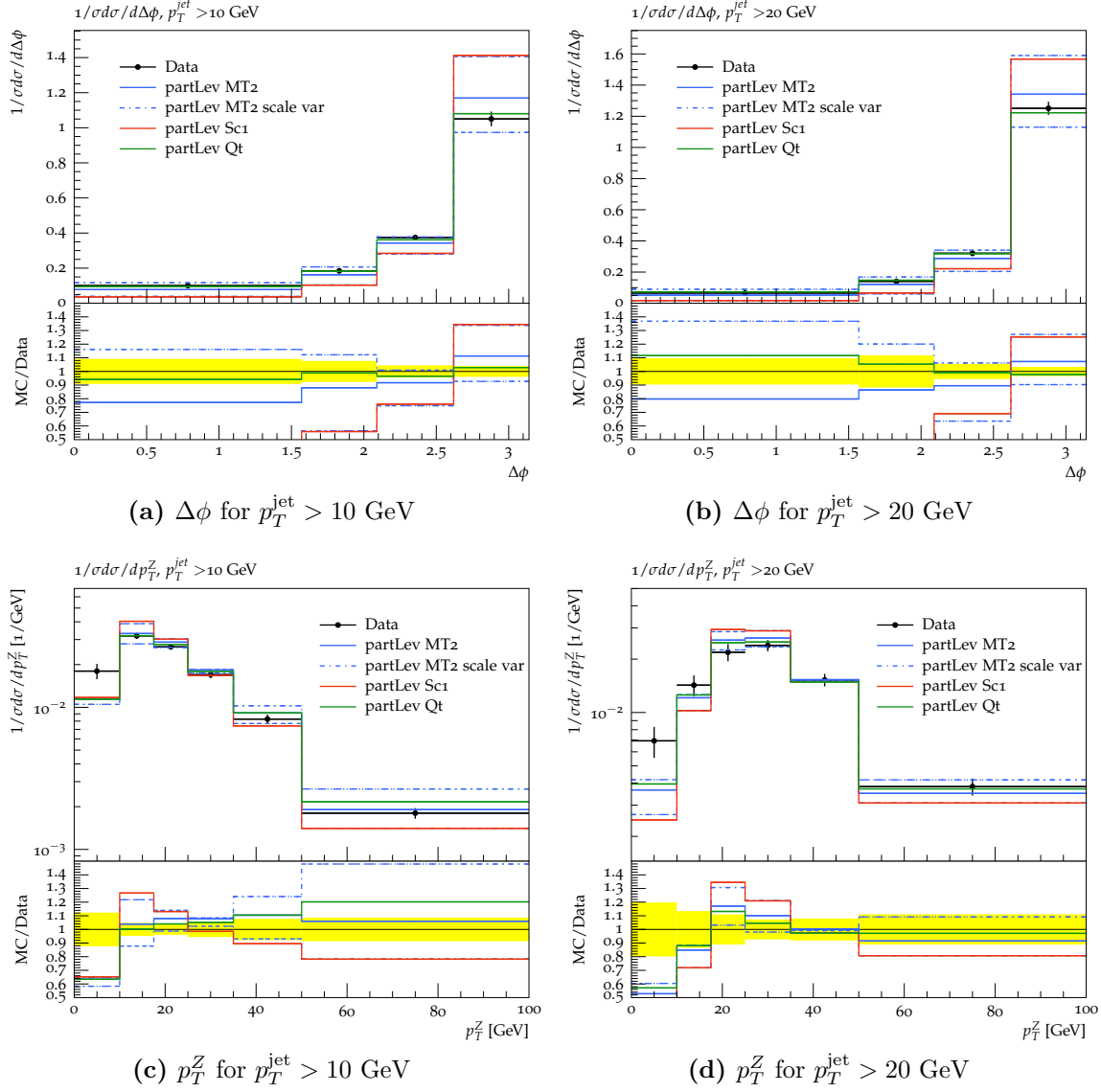


Figure 2: Comparison of different scale choices: MT2: $\mu = \sqrt{m_Z^2 + (p_T^{\text{jet}})^2}$, Sc1: $(p_T^{\text{jet}} + p_T^Z + m_Z)/3$, Qt: $\sqrt{\hat{s} + Q_t^2}$ for $\Delta\phi$ and p_T^Z distributions calculated at the parton level (without any showers). Compared to the LHCb measurements [12].

In Fig. 2 we investigate the importance of the scale choice by comparing the calculation with $\mu = \sqrt{m_Z^2 + (p_T^{\text{jet}})^2}$ (Fig. 1) with different choices: $\mu = (p_T^{\text{jet}} + p_T^Z + m_Z)/3$ and $\mu = \sqrt{\hat{s} + Q_t^2}$ with $Q_t = p_T^{\text{initial state}}$. We can see that the scale $\mu = \sqrt{\hat{s} + Q_t^2}$, which is motivated by angular ordering [29], gives results similar to our original scale choice, while the choice $\mu = (p_T^{\text{jet}} + p_T^Z + m_Z)/3$ leads to significant differences. However, most of the time the results are still within the scale uncertainty of the results from Fig. 1.

Based on this observation, we will use the scale $\mu = \sqrt{m_Z^2 + (p_T^{\text{jet}})^2}$ in the following.

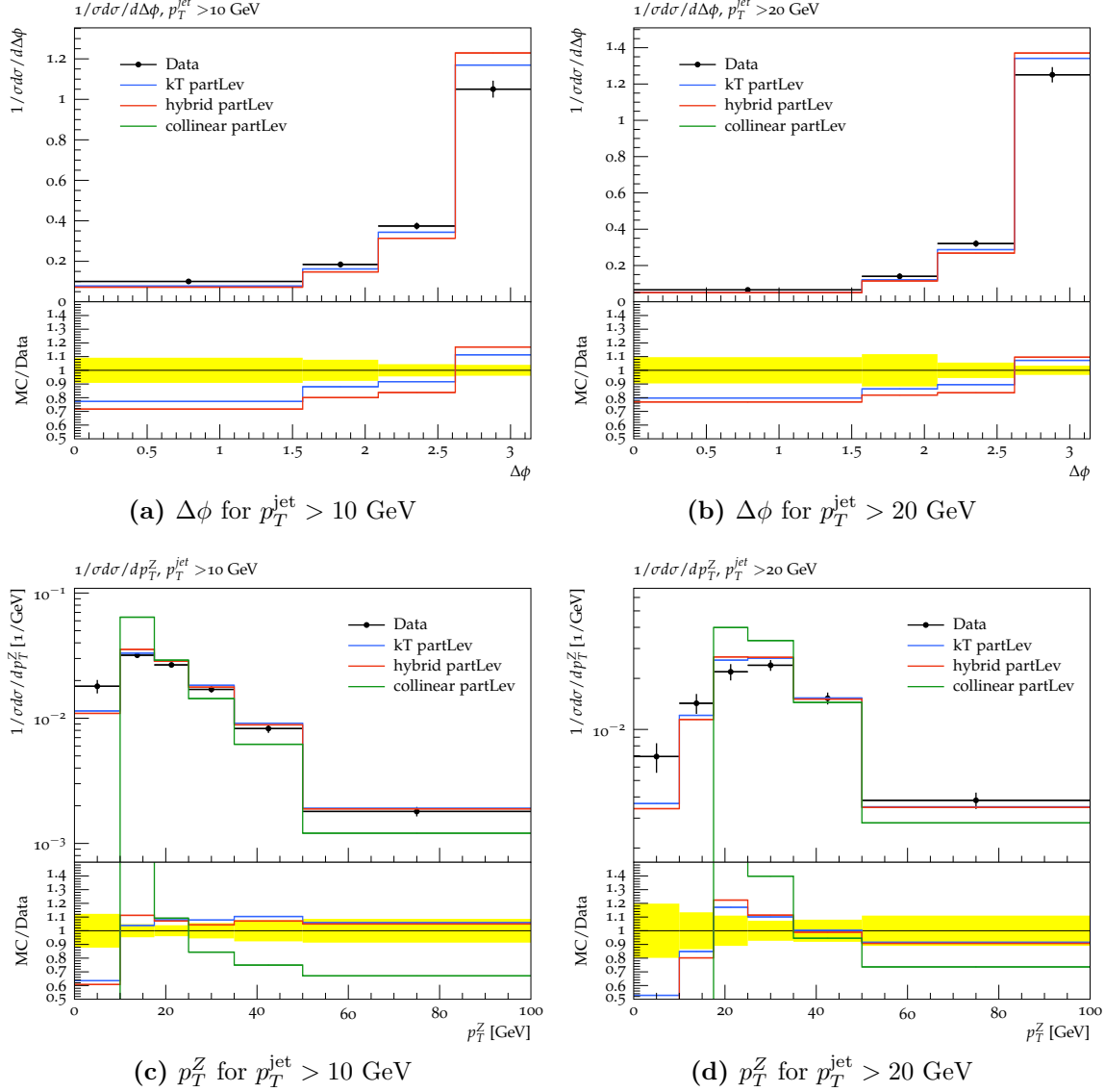


Figure 3: Comparison of $\Delta\phi$ and p_T^Z distributions calculated on parton level (without any showers) and the LHCb measurements [12]. The factorization/renormalization scale $\mu = \sqrt{m_Z^2 + (p_T^{\text{jet}})^2}$ is used for: k_T -factorization (two off-shell initial partons), hybrid factorization (one off-shell and one on-shell initial parton), and collinear factorization (two on-shell partons).

In Fig. 3 we compare the predictions obtained within k_T -factorization (presented in Fig. 1) to the corresponding predictions obtained in the hybrid (the lower x initial state parton is off-shell while the higher x initial state parton is on-shell) and collinear approaches at parton level. We can see that for both $\Delta\phi$ and p_T^Z distributions (with

both cut choices) the results of the hybrid approach are very similar to the ones of k_T -factorization. This shows that the hybrid factorization works well where it is expected to work, i.e. in the forward region where asymmetric values of x_1 and x_2 are probed. The key point in this study are the TMDs and collinear PDFs used: the k_T -integrated PB-TMD is identical to the collinear PDF by construction. When HE-factorization is used in the forward rapidity region, the k_T on the large x side is limited and the matrix elements with two off-shell initial state particles effectively become on-shell-off-shell, and in the process of evaluating the cross section the PDF on that side is integrated to yield a collinear PDF. In the hybrid factorization calculation, the collinear PDF was used from the beginning. A more detailed analysis of it will be provided in Sec. 2.3 where we discuss correlations of transverse momenta and x values of the initial partons.

In Fig. 3 we additionally present results obtained within collinear factorization. The motivation is to show that a purely collinear approach is not able to describe certain distributions at leading order (LO) and higher order corrections are needed. This is especially visible for the $\Delta\phi$ distribution which reduces to a delta function at LO. The cut on the p_T^{jet} restricts also the p_T^Z distribution since there is no recoil that would allow the Z boson to gain additional transverse momentum. Later we will compare our results also with predictions in collinear factorization at LO but including parton showers as well as with next-to-leading order (NLO) predictions.

2.2 Showered results

In this section we present results using an updated version of the CASCADE Monte Carlo event generator [10, 11, 30], allowing to process LHE Les Houches event files [31], generated by KATIE and to provide initial state parton showers according to the PB-TMDs. The calculations are also supplemented with standard final state parton shower and hadronization [23], the multi-parton interactions are not included. When off-shell matrix elements are used, the transverse momenta of the initial state partons are already included according to the TMDs. In case of collinear matrix elements, first a transverse momentum is generated according to the TMD and added to the event record in such a way, that the mass of the hard process \hat{s} is preserved, and the event is showered, while the parton shower does not change the kinematics of the hard process (after the transverse momentum is included). In hybrid factorisation, the initial state parton shower is included only for the off-shell leg, while the other leg stays at $k_T = 0$. It is important to stress, that the parton densities used in the calculations are applied in a consistent way.

In Fig. 4 we compare results obtained using k_T -factorization, hybrid factorization and collinear factorization (using the scale $\mu = \sqrt{m_Z^2 + (p_T^{\text{jet}})^2}$). We can see that, similarly to the results at the parton level, the k_T -factorization and hybrid factorization approaches give very similar results. On the other hand, we see a substantial change in the case of predictions from collinear factorization, which now is also quite similar to the other two predictions: the $\Delta\phi$ distribution in the collinear case is no longer zero and it gives a rather good description of the data. Note here that the $\Delta\phi$ distri-

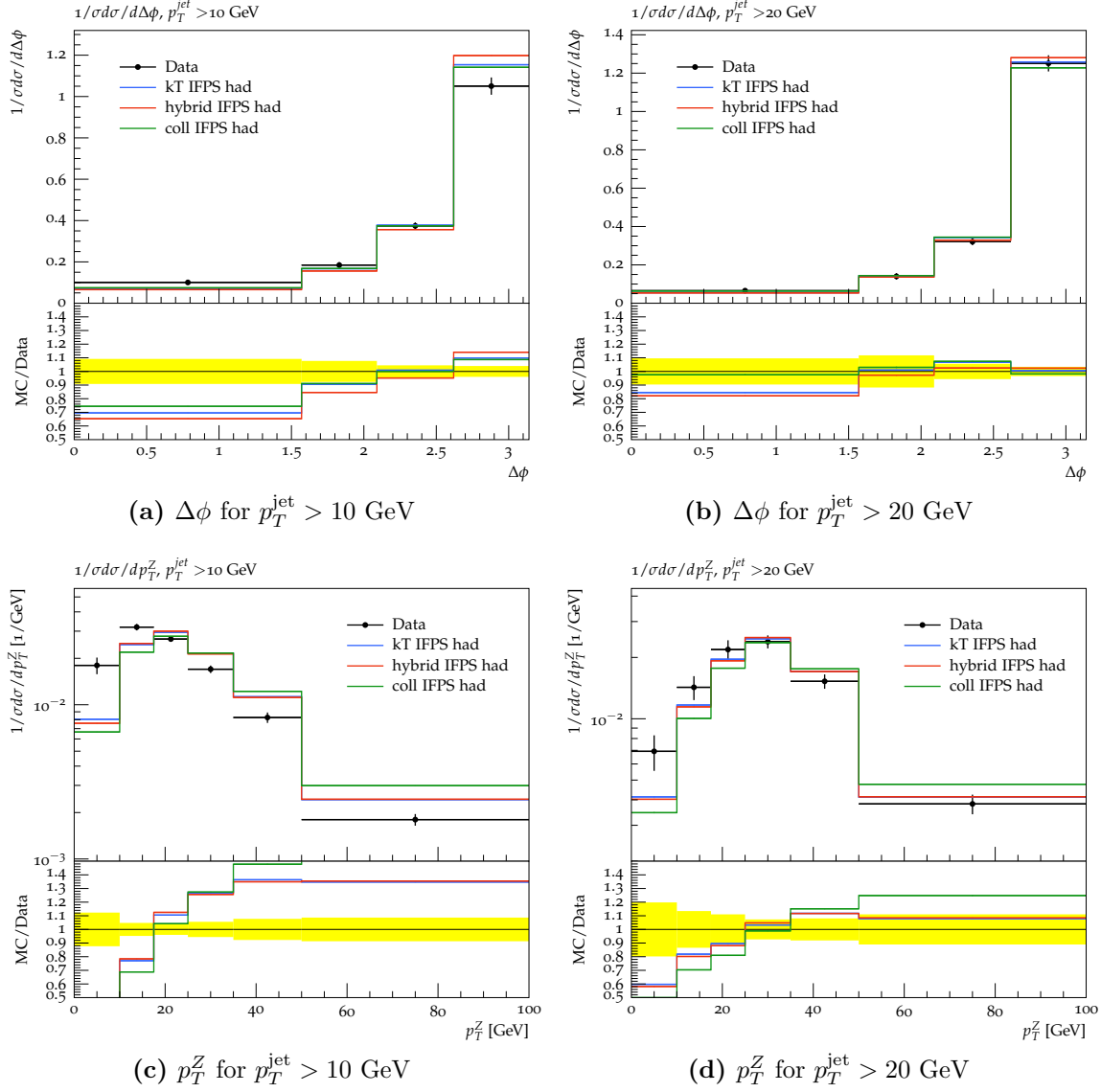


Figure 4: Comparison of $\Delta\phi$ and p_T^Z distributions calculated including initial and final state showers as well as hadronization, using factorization/renormalization scale $\mu = \sqrt{m_Z^2 + (p_T^{\text{jet}})^2}$ within: k_T -factorization (two off-shell initial partons), hybrid factorization (one off-shell and one on-shell initial parton), and collinear factorization (two on-shell partons). Compared to the LHCb measurements [12].

bution is fully generated by the TMDs (and the corresponding TMD shower). From a kinematic point of view this mimics the features of the off-shell calculation, where the initial transverse momenta are included from the beginning. It also points to the observation that initial state transverse momenta are perhaps more important than the off-shellness in the matrix elements: the off-shell matrix elements would contribute a dynamical correction, while the kinematics are driven by including the transverse

momenta from the TMDs. While calculations obtained in HE- and hybrid factorization give essentially the same results, a difference to results from collinear factorization with parton shower is observed. The parton densities and the parton showers are the same for all calculations, and the difference comes entirely from the different matrix elements used (off-shell versus on-shell).

The $\Delta\phi$ distributions are rather well described by all approaches, while in the p_T^Z dis-

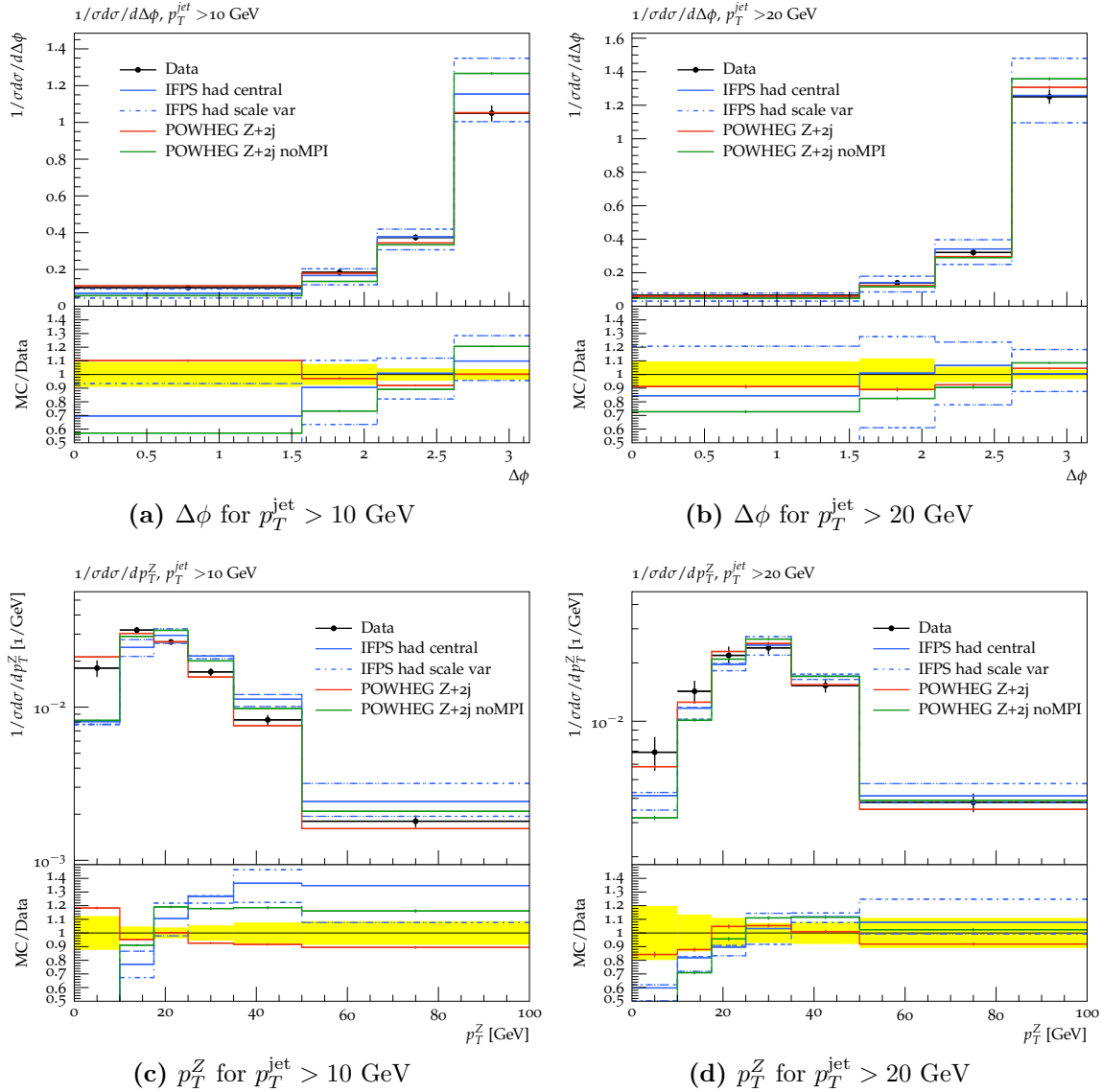


Figure 5: Scale variation for $\Delta\phi$ and p_T^Z distributions calculated including initial and final state showers as well as hadronization using factorization/renormalization scale $\mu = \sqrt{m_Z^2 + (p_T^{\text{jet}})^2}$ compared with POWHEG results for $Z + 2\text{jet}$ production. Compared to the LHCb measurements [12].

p_T^{jet} [GeV]	LHCb	k_T	hybrid	coll. (LO)	coll. (NLO) no MPI	coll. (NLO) with MPI
20	6.3 ± 0.55	$3.6 \pm 1 \cdot 10^{-5}$	$3.9 \pm 2 \cdot 10^{-5}$	$4.6 \pm 4 \cdot 10^{-5}$	5.2 ± 0.04	5.5 ± 0.4
10	16.0 ± 1.36	$7.5 \pm 2 \cdot 10^{-5}$	$7.9 \pm 4 \cdot 10^{-5}$	$9.1 \pm 7 \cdot 10^{-5}$	11.4 ± 0.09	15.5 ± 1.2

Table 1: Total cross-section for $Z + \text{jet}$ as measured by LHCb [12] and predicted by the corresponding calculations in k_T , hybrid and collinear factorization. All the calculations include showering and hadronization and were performed using the scale $\mu = \sqrt{m_Z^2 + (p_T^{\text{jet}})^2}$. The uncertainties of the theoretical predictions are numerical integration errors.

tribution, all approaches predict a too small cross section at small p_T^Z , the high-energy and hybrid factorization approach are slightly better than the collinear calculation with TMD showers included. We have checked that changing the scale μ gives similar effects as observed without TMD showers.

Finally, in Fig. 5 we compare k_T -factorization predictions with parton showers and hadronization (including scale variations by a factor of two) with a collinear NLO calculation of Z -boson and 2 jets performed in POWHEG (with MinLO method [32,33]), using the HERAPDF20_NLO collinear PDFs [27] and the PYTHIA8 tune CUETP8M1 [34]. We show predictions with and without multi-parton interactions (MPI). The measured $\Delta\phi$ distribution is well described by the NLO collinear calculation (Figs. 5a and 5b), when MPI is included. Similarly, the POWHEG calculation agrees rather well with the measured p_T^Z distribution (Figs. 5c and 5d), if MPI is included, in particular at small p_T^Z , below the p_T^{jet} cut-off. It is interesting to note, that at low p_T^Z the description of the measurement is significantly improved when MPI is included, meaning that some of the low p_T jets come from MPI. If the contribution from MPI is switched off, then the predictions calculated with collinear NLO $Z + 2$ jet and with off-shell matrix elements in LO k_T -factorization agree rather well. This observation confirms that the distributions using off-shell matrix elements are similar to the ones obtained by a collinear NLO calculation.

The differential distributions measured by LHCb are normalized to the total cross-section which means we could not judge the normalization of our predictions. In order to do it in Table 1 we show a comparison of the measured total cross-section with the different predictions. All LO predictions (using $\alpha_s(m_Z) = 0.118$) are significantly smaller than the measurements. This is partly caused by the use of NLO PDFs and 2-loop α_s . We have verified that using consistently LO PDFs and strong coupling (we used HERAPDF20_LO_EIG PDF set) increases the cross section and brings it closer to the measurement but it does not explain the whole difference.

Additionally, Table 1 shows us also the importance of the MPI for the total cross section.

2.3 Correlations

In this section we will analyse correlations between longitudinal and transverse components of the initial state partons.

In Fig. 6 the correlations between longitudinal momentum fractions of the initial state partons x_1 and x_2 are shown for both factorization schemes (HE and hybrid), for the region $20 < p_T^Z < 30$ GeV (results for other ranges of p_T^Z are similar). In the region of forward Z production, as defined by the LHCb measurement, one of the partons has a small longitudinal component ($x_2 \sim 10^{-3}$), whereas the second parton has rather large values $x_1 \sim 0.3$. In the hybrid approach, the initial off-shell parton is the one at low value of x , namely x_2 .

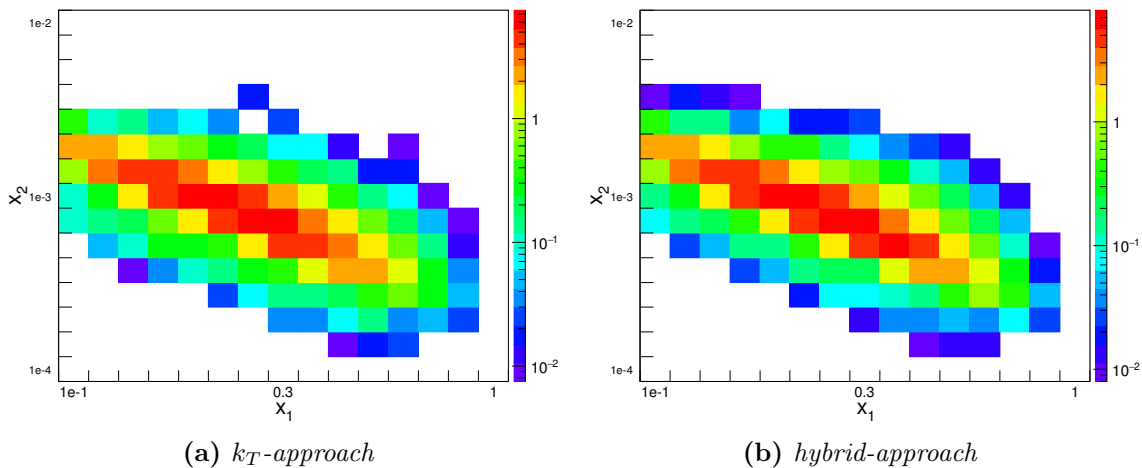


Figure 6: Correlation between longitudinal momentum fractions x of the initial state partons for a selected bin of Z boson transverse momentum: $20 < p_T^Z < 30$ GeV. Distributions for other bins in p_T^Z look similar.

In Fig. 7 the correlations between the transverse momenta of the initial state partons are shown for the case of k_T factorization (in the hybrid approach the k_{1T} momentum is zero).¹ One of the transverse momenta, k_{1T} (large x_1), is small ($k_{1T} \lesssim 5$ GeV), while the other one, k_{2T} (low x_2), has a much broader distribution. The average transverse momentum k_{2T} increases for increasing p_T^Z , as shown in Fig. 7, while the transverse momentum of the other parton stays very small. This observation explains why the predictions in HE (two off-shell partons) and hybrid factorization (only one off-shell parton) give very similar results.

In Fig. 8 the correlation between the longitudinal and the transverse momentum of the low energetic parton is shown, for both k_T -factorization and hybrid factorization approaches. With increasing transverse momentum of the Z -boson, the longitudinal

¹The scale for all the color-map plots is the same as in Fig. 6.

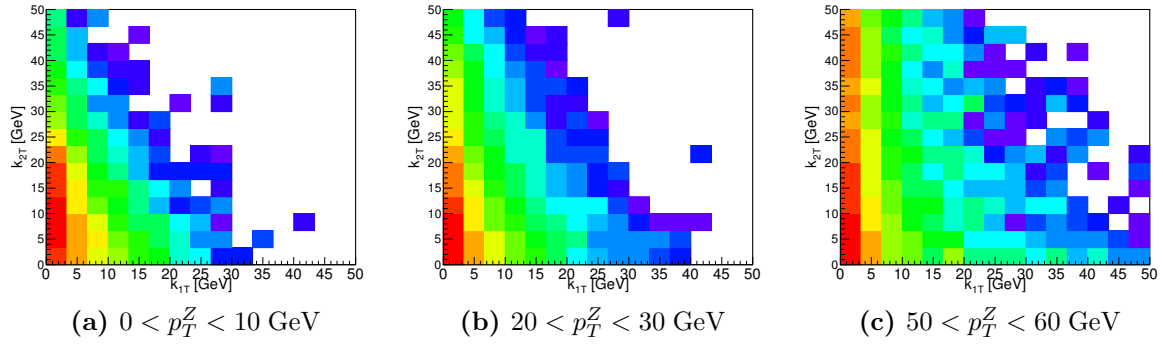


Figure 7: Correlation between transverse momenta of the initial state partons k_{1T} (with large x value) and k_{2T} (with low x value) for selected bins of Z boson transverse momentum for the high-energy approach.

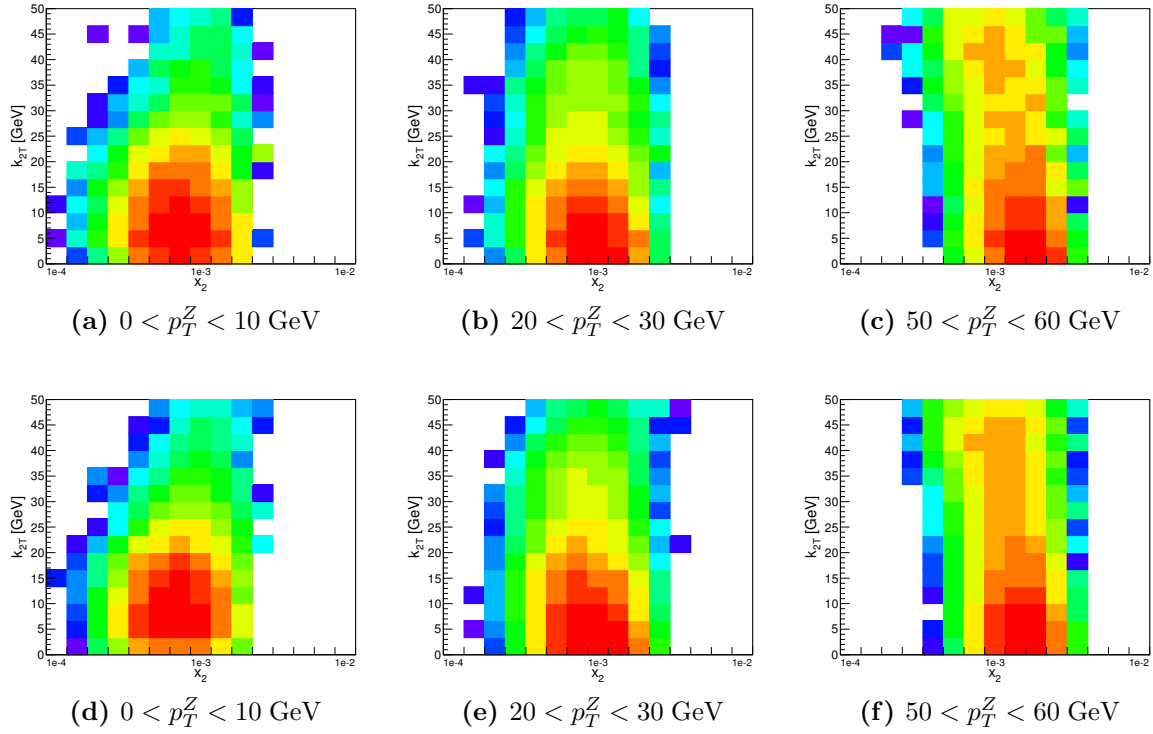


Figure 8: Correlation between longitudinal momentum fraction x_2 and transverse momentum of the second initial state parton k_{2T} (low longitudinal momentum fraction) for selected bins of the Z boson transverse momentum. The upper row displays results for k_T -factorization, lower row for the hybrid approach.

momentum x_2 also increases. Both factorization approaches show very similar correlations between x_2 and k_{2T} as a function of p_T^Z , confirming again the equivalence of

k_T -factorization and hybrid factorization results in the region of forward Z production.

3 Conclusion

We have presented calculations of $Z+1$ jet final states including transverse momenta of the initial state partons and compared the predictions with measurements of the LHCb experiment. The calculations were performed using the KATIE parton-level event generator together with initial state parton showers implemented in a new version of CASCADE. We have applied consistently the parton branching transverse momentum dependent parton densities (PB-TMDs) together with two-loop $\alpha_s(m_Z) = 0.118$.

The predictions obtained in high-energy and hybrid factorization agree very well with each other for the forward Z production pointing towards effective equivalence of the two approaches in the forward region. The predictions obtained in collinear factorization at leading order for $Z+1$ jet, supplemented with PB-TMDs and corresponding parton shower show differences to predictions obtained in high-energy factorization, which come from the different matrix elements used. A comparison of prediction obtained in high-energy factorisation and a collinear NLO calculation of $Z+2$ jet supplemented with standard parton showers shows very good agreement. The description of the experimental measurement especially at very small p_T^Z is significantly improved when contributions from multi-parton interactions are included.

The predictions obtained in high-energy factorisation (as well as in hybrid factorization) agree rather well with the measurements of the LHCb collaboration. Differences are observed in the region of small p_T^Z , where the predictions depend significantly on the treatment of multi-parton interactions, which are not yet included in the calculations with high-energy factorization.

We have presented a first consistent comparison of calculations in different factorization approaches, and illustrate the features and advantages of using off-shell matrix elements obtained in k_T -factorization.

Acknowledgments

Krzysztof Kutak acknowledges the support of Narodowe Centrum Nauki with grant DEC-2017/27/B/ST2/01985. Michal Deak, Andreas van Hameren and Aleksander Kusina acknowledge the support by FWO-PAS VS.070.16N research grant. Andreas van Hameren was also partially supported by grant of National Science Center, Poland, No. 2015/17/B/ST2/01838. Mirko Serino is supported by the Israeli Science Foundation through grant 1635/16, by the BSF grants 2012124 and 2014707, by the COST Action CA15213 THOR and by a Kreitman fellowship by the Ben Gurion University of the Negev. Hannes Jung thanks the Polish Science Foundation for the Humboldt Research fellowship during which part of this work was completed.

References

- [1] F. Hautmann, M. Hentschinski, and H. Jung, “Forward Z-boson production and the unintegrated sea quark density,” *Nucl. Phys.* **B865** (2012) 54–66, [1205.1759](#).
- [2] L. Motyka, M. Sadzikowski, and T. Stebel, “Twist expansion of Drell-Yan structure functions in color dipole approach,” *JHEP* **05** (2015) 087, [1412.4675](#).
- [3] A. van Hameren, P. Kotko, and K. Kutak, “Resummation effects in the forward production of Z₀+jet at the LHC,” *Phys. Rev.* **D92** (2015), no. 5, 054007, [1505.02763](#).
- [4] W. Schfer and A. Szczurek, “Drell-Yan production at forward rapidities: a hybrid factorization approach,” in *24th Low-x Meeting (Low-x 2016) Gyongyos, Hungary, June 6-10, 2016*. 2016. [1610.05123](#).
- [5] F. G. Celiberto, D. Gordo Gmez, and A. Sabio Vera, “Forward Drell-Yan production at the LHC in the BFKL formalism with collinear corrections,” [1808.09511](#).
- [6] R. Angeles-Martinez *et al.*, “Transverse Momentum Dependent (TMD) parton distribution functions: status and prospects,” *Acta Phys. Polon.* **B46** (2015), no. 12, 2501–2534, [1507.05267](#).
- [7] M. Deak, F. Hautmann, H. Jung, and K. Kutak, “Forward-Central Jet Correlations at the Large Hadron Collider,” [1012.6037](#).
- [8] S. Catani, M. Ciafaloni, and F. Hautmann, “High-energy factorization and small x heavy flavor production,” *Nucl. Phys.* **B366** (1991) 135–188.
- [9] A. van Hameren, “KaTie : For parton-level event generation with k_T -dependent initial states,” *Comput. Phys. Commun.* **224** (2018) 371–380, [1611.00680](#).
- [10] H. Jung, S. Baranov, M. Deak, A. Grebenyuk, F. Hautmann, *et al.*, “The CCFM Monte Carlo generator CASCADE version 2.2.03,” *Eur.Phys.J.* **C70** (2010) 1237, [1008.0152](#).
- [11] M. Bury, A. van Hameren, H. Jung, K. Kutak, S. Sapeta, and M. Serino, “Calculations with off-shell matrix elements, TMD parton densities and TMD parton showers,” *Eur. Phys. J.* **C78** (2018), no. 2, 137, [1712.05932](#).
- [12] **LHCb** Collaboration, R. Aaij *et al.*, “Study of forward Z + jet production in pp collisions at $\sqrt{s} = 7$ TeV,” *JHEP* **01** (2014) 033, [1310.8197](#).
- [13] P. Kotko, K. Kutak, C. Marquet, E. Petreska, S. Sapeta, and A. van Hameren, “Improved TMD factorization for forward dijet production in dilute-dense hadronic collisions,” *JHEP* **09** (2015) 106, [1503.03421](#).

- [14] A. van Hameren, P. Kotko, K. Kutak, C. Marquet, E. Petreska, and S. Sapeta, “Forward di-jet production in p+Pb collisions in the small-x improved TMD factorization framework,” *JHEP* **12** (2016) 034, [1607.03121](#).
- [15] A. van Hameren, P. Kotko, and K. Kutak, “Multi-gluon helicity amplitudes with one off-shell leg within high energy factorization,” *JHEP* **12** (2012) 029, [1207.3332](#).
- [16] A. van Hameren, P. Kotko, and K. Kutak, “Helicity amplitudes for high-energy scattering,” *JHEP* **01** (2013) 078, [1211.0961](#).
- [17] E. N. Antonov, L. N. Lipatov, E. A. Kuraev, and I. O. Cherednikov, “Feynman rules for effective Regge action,” *Nucl. Phys.* **B721** (2005) 111–135, [hep-ph/0411185](#).
- [18] M. A. Kimber, A. D. Martin, and M. G. Ryskin, “Unintegrated parton distributions,” *Phys. Rev.* **D63** (2001) 114027, [hep-ph/0101348](#).
- [19] A. D. Martin, M. G. Ryskin, and G. Watt, “NLO prescription for unintegrated parton distributions,” *Eur. Phys. J.* **C66** (2010) 163–172, [0909.5529](#).
- [20] F. Hautmann, H. Jung, A. Lelek, V. Radescu, and R. Zlebcik, “Collinear and TMD quark and gluon densities from Parton Branching solution of QCD evolution equations,” *JHEP* **01** (2018) 070, [1708.03279](#).
- [21] F. Hautmann, H. Jung, A. Lelek, V. Radescu, and R. Zlebcik, “Soft-gluon resolution scale in QCD evolution equations,” *Phys. Lett.* **B772** (2017) 446, [1704.01757](#).
- [22] A. Bermudez Martinez, P. Connor, F. Hautmann, H. Jung, A. Lelek, V. Radescu, and R. Zlebcik, “Collinear and TMD parton densities from fits to precision DIS measurements in the parton branching method,” [1804.11152](#).
- [23] T. Sjöstrand, S. Mrenna, and P. Skands, “PYTHIA 6.4 physics and manual,” *JHEP* **05** (2006) 026, [hep-ph/0603175](#).
- [24] B. Jager, S. Schneider, and G. Zanderighi, “Next-to-leading order qcd corrections to electroweak zjj production in the powhegbox,” [1207.2626v1](#).
- [25] T. Sjöstrand, S. Ask, J. R. Christiansen, R. Corke, N. Desai, P. Ilten, S. Mrenna, S. Prestel, C. O. Rasmussen, and P. Z. Skands, “An introduction to PYTHIA 8.2,” *Comput. Phys. Commun.* **191** (2015) 159, [1410.3012](#).
- [26] F. Hautmann, H. Jung, M. Krämer, P. J. Mulders, E. R. Nocera, T. C. Rogers, and A. Signori, “TMDlib and TMDplotter: library and plotting tools for transverse-momentum-dependent parton distributions,” *Eur. Phys. J.* **C74** (2014) 3220, [1408.3015](#).

- [27] **ZEUS, H1** Collaboration, H. Abramowicz *et al.*, “Combination of measurements of inclusive deep inelastic $e^\pm p$ scattering cross sections and QCD analysis of HERA data,” *Eur. Phys. J.* **C75** (2015), no. 12, 580, [1506.06042](#).
- [28] A. Buckley, J. Butterworth, L. Lonnblad, D. Grellscheid, H. Hoeth, J. Monk, H. Schulz, and F. Siegert, “Rivet user manual,” *Comput. Phys. Commun.* **184** (2013) 2803–2819, [1003.0694](#).
- [29] H. Jung, “ $k(t)$ -factorization and CCFM: The solution for describing the hadronic final states - everywhere?,” *Mod. Phys. Lett.* **A19** (2004) 1–18, [hep-ph/0311249](#).
- [30] H. Jung, “The CCFM Monte Carlo generator CASCADE,” *Comput. Phys. Commun.* **143** (2002) 100, [hep-ph/0109102](#).
- [31] J. Alwall *et al.*, “A standard format for Les Houches event files,” *Comput. Phys. Commun.* **176** (2007) 300, [hep-ph/0609017](#).
- [32] K. Hamilton, P. Nason, and G. Zanderighi, “MINLO: Multi-Scale Improved NLO,” *JHEP* **10** (2012) 155, [1206.3572](#).
- [33] K. Hamilton, P. Nason, C. Oleari, and G. Zanderighi, “Merging H/W/Z + 0 and 1 jet at NLO with no merging scale: a path to parton shower + NNLO matching,” *JHEP* **05** (2013) 082, [1212.4504](#).
- [34] **CMS** Collaboration, V. Khachatryan *et al.*, “Event generator tunes obtained from underlying event and multiparton scattering measurements,” *Eur. Phys. J.* **C76** (2016), no. 3, 155, [1512.00815](#).